

# Canalization in the Critical States of Highly Connected Networks of Competing Boolean Nodes

Matthew D. Reichl<sup>1,2</sup> and Kevin E. Bassler<sup>1,2</sup>

<sup>1</sup>*Department of Physics, University of Houston, Houston, Texas 77204-5005, USA*

<sup>2</sup>*Texas Center for Superconductivity, University of Houston, Houston, Texas 77204-5002, USA*

(Dated: June 15, 2011)

Canalization is a classic concept in Developmental Biology that is thought to be an important feature of evolving systems. In a Boolean network it is a form of network robustness in which a subset of the input signals control the behavior of a node regardless of the remaining input. It has been shown that Boolean networks can become canalized if they evolve through a frustrated competition between nodes. This was demonstrated for large networks in which each node had  $K = 3$  inputs. Those networks evolve to a critical steady-state at the border of two phases of dynamical behavior. Moreover, the evolution of these networks was shown to be associated with the symmetry of the evolutionary dynamics. We extend these results to the more highly connected  $K > 3$  cases and show that similar canalized critical steady states emerge with the same associated dynamical symmetry, but only if the evolutionary dynamics is biased toward homogeneous Boolean functions.

PACS numbers: 89.75.Fb, 87.23.Kg, 05.65.+b, 89.75.Hc

## I. INTRODUCTION

Boolean networks were originally proposed as models of genetic regulatory networks and are now widely used as models of self-regulatory behavior in biological, physical, social, and engineered systems [1–4]. They are designed to capture essential features of the complex dynamics of real networks by “coarse-graining” that assumes that dynamical state of each node is Boolean, or simply on/off [5]. For example, in a model of a genetic regulatory system each node corresponds to a gene and its Boolean dynamical state refers to whether or not the gene is currently being expressed. The regulatory interactions between nodes are described by a directed graph in which the Boolean (output) state of each node is determined by a function of the states of the nodes connected to it with directed in-links. It has been shown that, despite their simplicity, Boolean networks capture many of the important features of the dynamics of real self-regulating networks, including biological genetic circuits [6–9].

Perhaps the most notable feature of Boolean networks is that they have two distinct phases of dynamical behavior. These two phases are called “frozen” and “chaotic”, and in random Boolean networks there is a continuous phase transition between them [10–12]. The two phases can be distinguished by how a perturbation in the network spreads with time: in the frozen phase a perturbation decays with time, while in the chaotic phase a perturbation grows with time [10, 13]. In networks in which the states of the nodes are updated synchronously, the two phases can also be distinguished by the distribution of network’s attractor periods [3, 14]. When the updates are synchronous the system always settles onto a dynamical attractor of finite period. In the frozen phase the distribution of attractor periods is sharply peaked with a mean that is independent of the number of nodes  $N$ . In the chaotic phase the distribution of attractor periods

is also sharply peaked, but with a mean that grows as  $\exp(N)$ . In the “critical” state, at the boundary between the two phases, the distribution of attractor periods is broad, described by a power-law [14–17].

Many naturally occurring, as well as engineered, self-regulating network systems develop through some sort of evolutionary process. Motivated by this fact, a number of models that evolve the structure and dynamics of Boolean networks have been studied [17–32]. These evolutionary Boolean network (EBN) models generally seek to determine the properties of networks that result from the evolutionary mechanism being considered. For example, some studies have explored evolutionary mechanisms that result in networks that have dynamics that are robust against various types of perturbations, or that result in networks that are in a critical state.

One example of an EBN is the model of competing Boolean nodes first introduced in Ref. [17], and later studied in Refs. [23, 24, 26]. In this model, the Boolean functions of the nodes evolve through a frustrated competition for limited resources between nodes that is a variant of the Minority game [33]. In the original paper on the model, it was shown that the network self-organizes to a nontrivial critical state with this evolutionary mechanism. Later it was discovered that this critical state is highly canalized [23]. Canalization [34] is a type of network robustness, and is a classic idea in developmental biology. Recently, experiments have demonstrated its existence in genetic regulatory networks [35–37]. It occurs when certain expression states of only a subset of genes that regulate the expression of a particular gene control the expression of that gene. Canalization is thought to be an important property of developmental biological systems because it buffers their evolution, allowing greater underlying variation of the genome and its regulatory interactions before some deleterious variation can be expressed phenotypically [38]. Critical net-

works are thought to be important for gene regulation because they can store and transfer more information than either frozen networks, which have a static output, or chaotic networks, which have a random output [2].

In the previous studies of the EBN with competing nodes, it was found that, for large networks in which each node has  $K = 3$  in-links, the system evolves to a steady state that is both critical and highly canalized. The canalized nature of the evolved state was found by measuring the average frequency at which each of the 256 possible Boolean functions of three variables occur. It was discovered that the functions organize into 14 different classes in which all of the functions in each class occur with approximately the same frequency. Moreover, all functions in a class are equally canalizing and the classes whose functions are more canalizing occur with higher frequency. It was then found that the existence of these 14 classes is due to the symmetry properties of the evolutionary dynamics [39].

In this paper, we extend these results to more highly connected Boolean networks in which nodes have  $K > 3$  in-links. We show that, although an unbiased implementation of the same evolutionary process does not lead to a critical state as it does for  $K = 3$ , by biasing the process in a way that encourages the evolution of more homogeneous functions the system can evolve to a critical steady state. We also show that the possible Boolean functions again organize into classes that depend on the symmetry of the evolutionary dynamics and that all functions in a class occur with the same average frequency. In this case however, the bias added to the evolutionary process causes a competition between the preference for canalization and a preference for homogeneity induced by the bias. This competition between canalization and homogeneity is reflected in the frequency at which the Boolean functions occur.

## II. THE MODEL

### A. Random Boolean Networks

A Random Boolean Network (RBN) consists of  $N$  nodes,  $i = 1, \dots, N$ , each of which have a dynamical state with Boolean value  $\sigma_i = 0$  or 1. The Boolean state of each node is a function of the Boolean valued states of a set of  $K_i$  other randomly chosen nodes that regulate it. The regulatory interactions of the nodes are, thus, described by a directed graph. For synchronously updating Boolean networks, which are the only ones considered here, the states  $\sigma_i$  at time  $t + 1$  is a function of all states of its  $K_i$  regulatory nodes  $\{i_1, i_2, \dots, i_{K_i}\}$  at time  $t$ :

$$\sigma_i(t + 1) = f_i[\sigma_{i_1}(t), \sigma_{i_2}(t), \dots, \sigma_{K_i}(t)] \quad (1)$$

The function  $f_i$  is a Boolean function of  $K_i$  inputs that determines the output of node  $i$  for all  $2^{K_i}$  possible sets of input values. In this particular study, we consider

RBNs in which  $K_i$  is fixed for all nodes  $i$ . No self-links, or multiple in-links from the same node are allowed in our models.

In RBNs, each of the different functions  $f_i$  is chosen randomly. We do this by choosing the  $2^K$  outputs of each of the  $N$  functions either to be ‘0’ with probability  $p$  and ‘1’ with probability  $1-p$ , or to be ‘0’ with probability  $1-p$  and ‘1’ with probability  $p$ . Which of the two cases is used is chosen with equal probability for each function  $f_i$ , but remains fixed while assigning all of the individual outputs to that particular function. By choosing the Boolean functions in this way, a symmetry between ‘0’s and ‘1’s exists on average in the network. Note that the effective range of  $p$  is only from 0.5 to 1.

Note that if  $p = 1/2$ , the choice of functions is unbiased and each of the  $2^{2^K}$  functions are equally likely to be chosen. For  $p \neq 1/2$  the choice of functions is biased toward homogeneity. The homogeneity of a function  $f_i$  is defined as the probability that it will output a “0”, or the probability that it will receive a “1”, whichever is larger, assuming that it receives random input. The average homogeneity of the network,  $P$ , is the average homogeneity over the functions of all nodes  $i$ .

The system state  $\Sigma$  of the network at time  $t$  is given by the array of Boolean values of the states of each node:

$$\Sigma(t) = \{\sigma_1(t), \dots, \sigma_N(t)\} \quad (2)$$

Because the dynamics prescribed in Eq. 1 are deterministic, and the space of all possible network states is finite (of size  $2^N$ ), all dynamical trajectories eventually become periodic. That is, after some possible transient behavior, each trajectory will repeat itself after some number of discrete time steps  $\Gamma$  to form a periodic cycle given by:

$$\Sigma(t) = \Sigma(t + \Gamma) \quad (3)$$

The periodic trajectory over this cycle is referred to as the “attractor” of the dynamics, and the minimum  $\Gamma$  that satisfies this equation is the “period” of the attractor.

As mentioned above, two distinct phases of dynamical behavior, “frozen” and “chaotic”, exist for RBNs. For networks with uniform  $K > 2$ , networks are in the chaotic phase when  $p$  is near 0.5 and in the frozen or “fixed” phase when  $p$  is near 0 or 1. There is a continuous phase transition between these phases at the so called “edge of chaos.” The critical value  $p_c$  where this transition occurs satisfies the expression [10–12]

$$1 = 2Kp_c(1 - p_c) \quad (4)$$

We will refer to the networks that are critical because they satisfy Eq. 4 by construction as “non-evolutionary” networks, since such networks have no evolutionary dynamics associated with them.

### B. Evolutionary Game of Competing Nodes

The process for evolving the Boolean functions in the network is:

1. Start with an RBN constructed with a bias  $p$ , and choose a random initial state  $\Sigma(0)$ .
2. Update the state of the network using Eq. 1, and determine the attractor of the dynamics. (The attractor can be found using the algorithm discussed in the Appendix of Ref. 25.)
3. For each update on the attractor, determine which Boolean value is the output state of the majority of the nodes, and give a point to each node that is part of the majority.
4. Determine the node with the largest number of points; that node “loses”. If two, or more, nodes are tied, pick one at random to be the loser.
5. Replace the function of the losing node with a new randomly chosen Boolean function with bias  $p$ .
6. Return to step 2.

The essential features of the game are (1) frustration [33, 40], since most nodes lose each time step, (2) negative reinforcement, since losing behavior is punished, and (3) extremal dynamics [41], since only the worst performing nodes Boolean function is changed.

Note that previous studies of this evolutionary model have always replaced the function of the losing node with an unbiased,  $p = 0.5$  random Boolean function. Thus, the evolutionary game we study here differs from previous work only at step 5.

If the attractor period is longer than some limiting time,  $\Gamma_{\max}$ , then the score is kept only over that limited time. In our simulations,  $\Gamma_{\max} = 10^4$  was used. Each progression through the game is called an “epoch”.

In this evolutionary process only the Boolean functions evolve; the directed network describing the regulatory interactions between nodes does not change. However, as we will see, canalization effectively removes interactions from the network. Thus, as the Boolean functions evolve and canalization increases the directed network of regulatory interactions effectively changes [39]. Thus, effectively, both the structure of the network and the dynamics of the nodes simultaneously evolve, making the model effectively a co-evolving adaptive network model [20, 42].

### III. CANALIZATION AND SYMMETRY

#### A. Canalization and Ising Hypercubes

As mentioned above, for large networks with  $K = 3$ , it has been found [23, 26] that the  $256 = 2^{2^K}$  possible Boolean functions of three variables organize into 14 different classes in which the functions belonging to each class occur with the same frequency in the critical steady-state that results from the evolutionary game. Moreover, all the functions in a class are equally canalizing, and, in the steady state, functions in classes that are more

canalizing occur with higher frequency. Thus, for  $K = 3$  the game causes networks to evolve to a critical steady state that is highly canalized. Canalization occurs in Boolean networks when the Boolean functions assigned to the nodes are canalizing. A Boolean function is canalizing if its output is fully determined by a specific value of one, or more of its inputs, regardless of the value of the other inputs. The canalization of a function can be quantified by a set of numbers  $\mathbf{P}_k$ ,  $k = 0, 1, \dots, K - 1$ , which are defined as the fraction of the different possible sets of  $k$  input values that are canalizing [2].

Canalization can be further understood by mapping Boolean functions of  $K$  inputs onto configurations, or “colorings”, of the  $K$ -dimensional Ising hypercube [39]. The Ising hypercube is a hypercube which has each vertex labeled, or colored, either ‘0’ or ‘1’ (“black” or “white”). In this representation, each of the  $2^K$  possible sets of input values corresponds to coordinates on a given axis of the hypercube. The color of each vertex represents the output value of the function for the associated input values. The mapping of a Boolean function of  $K$  inputs to a configuration of the  $K$ -dimensional hypercube is one-to-one.

This representation of Boolean functions as colorings of Ising hypercubes facilitates quick recognition of canalizing functions. For a  $K$ -dimensional hypercube, the fractions of canalizing inputs  $\mathbf{P}_k$  of a Boolean functions are the fraction of its  $K - k$  dimensional hypersurfaces that are homogeneously colored.

#### B. Symmetry of Evolutionary Dynamics

This Ising hypercube representation is particularly helpful for understanding the role of symmetry in the evolutionary dynamics. The fourteen (14) different classes that were observed empirically in the original  $K = 3$  study were later recognized as being those Ising hypercube colorings that are related by cubic symmetry plus parity [39]. Parity in this case refers to simultaneously inverting the Boolean values associated with each vertices. An underlying symmetry of the evolutionary dynamics was therefore reflected in this symmetry of the evolved steady-state. Furthermore, this symmetry preserves the canalization values  $\mathbf{P}_k$  of functions in each class, since neither cubic nor parity operations change the percentage of homogeneously colored hypersurfaces.

In mathematical terms the different classes correspond to the group orbits of the “Zyklenzeiger” group, which is the hyper-octahedral symmetry group  $O_n$  (where  $n = K$ ) combined with parity [39]. A group orbit is the set of configurations that map into each other through applications of a group’s symmetry operations. The number of orbits  $P_G$  can be calculated analytically using Pólya’s theorem [43]:

$$P_G = \frac{1}{|G|} \sum_{g \in G} |X^g| \quad (5)$$

where  $G$  is the symmetry group acting on the  $K$ -dimensional Ising hypercube,  $|G|$  is the number of operators  $g \in G$ ,  $X$  is the set of hypercube colorings,  $X^g$  is the set of colorings that are left invariant by  $g$ , and  $|X^g|$  is the size of set  $X^g$ .

To apply this theorem, one must construct all the operators of the group, sum the number of functions left invariant by each operator, and divide by the total number of symmetry operators. The hyper-octahedral group  $O_n$  has  $n!2^n$  operations. Including parity operations doubles this number.

A given symmetry operator  $g$  can be written as a permutation of the vertex numbers on a given hypercube. As a result, each operator  $g$  can be expressed in terms of its cycle structure  $x_1^{b_1} x_2^{b_2} \dots x_m^{b_m}$ , where  $\sum_{i=0}^m i b_i = 2^K$ . This notation indicates that  $g$  contains  $b_1$  cycles of length 1,  $b_2$  cycles of length 2, etc. The complete cycle representation of the hyper-octahedral group for an arbitrary dimension  $K$  is given by a known recursion relation [44]. For  $K = 3$  the complete cycle relation is:

$$x_1^8 + 13x_2^4 + 8x_1^2 x_3^2 + 8x_2 x_6 + 6x_1^4 x_2^2 + 12x_4^2 \quad (6)$$

where the coefficients of this polynomial indicate the number operators with a particular cycle structure.

Without parity, the number of functions left invariant is equal to  $2^{N_c}$ , where  $N_c = \sum_{i=1}^m b_i$  is the total number of cycles in the operator. Parity must be treated separately; no functions are left invariant by the parity operator with any hyper-octahedral operator containing at least one cycle of length 1. Thus there are  $2^{N_p}$  functions left invariant for the operators which include parity, where  $N_p = (1 - \Theta(b_1)) \sum_{i=1}^m b_i$  and  $\Theta$  is the Heaviside step function.

Thus, applying Pólya's theorem to the  $K = 3$  case, we arrive at

$$P_G = (1/96)((2)^8 + 13(2)^4 + 13(2)^4 + 8(2)^4 + 8(2)^2 + 8(2)^2 + 6(2)^6 + 12(2)^2 + 12(2)^2) = 14 \quad (7)$$

This is precisely how many function classes were found empirically in the  $K = 3$  case [23, 39]. Similarly, the complete cycle representation for the  $K = 4$  is

$$x_1^{16} + 12x_1^8 x_2^4 + 51x_2^8 + 12x_1^4 x_2^6 + 32x_1^4 x_3^4 + 48x_1^2 x_2 x_4^3 + 84x_4^4 + 96x_2^2 x_6^2 + 48x_8^2 \quad (8)$$

Using this result, accounting for parity, and applying Pólya's theorem we calculate  $P_G = 222$  for a 4-dimensional hypercube under rotation plus parity symmetry. (Note that an erroneous value of  $P_G = 238$  was reported in Ref. [39].) This is how many classes of functions should be observed in a critical steady state of  $K = 4$  networks undergoing the evolutionary dynamics. Below we show that results from numerical simulations are consistent with this prediction. Moreover, the frequencies that these functions occur show a preference for canalization.

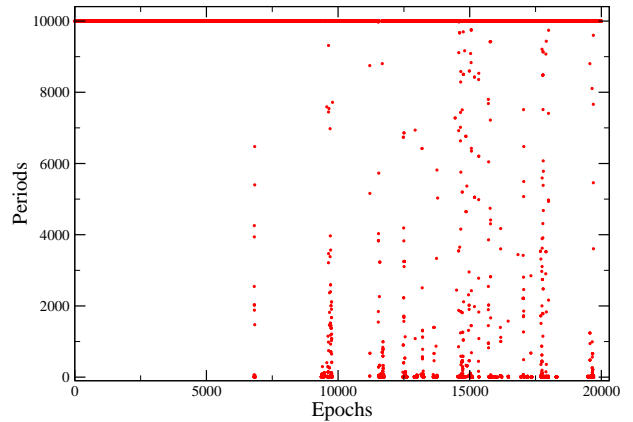


FIG. 1: (Color online) A graph of attractor period vs. epochs for a simulation of a  $K = 4$  network realization with an evolutionary bias of  $p = 0.65$ . Notice that neither short periods nor long periods dominate the behavior after the steady state is reached at  $\approx 10^4$  epochs.

## IV. RESULTS

### A. Critical States of $K=4$ Networks with Competing Nodes

We have performed exhaustive simulations of ensembles of networks with  $K = 4$  playing the game of competing Boolean nodes. All of the simulation results reported in this subsection are for networks with  $N = 999$  nodes. Simulations were run for evolutionary processes with biases of  $p = 0.5$ ,  $p = 0.65$ , and  $p = 0.75$ . The frequency that each of the  $2^{2^K} = 65536$  different functions occurred in the evolved steady state was measured by simulating, for each  $p$ , an ensemble of 13,000 independent network realizations. Each realization was initialized with an independent random network with random links and different random functions biased with the associated  $p$  value. The simulation of each realization was run for  $10^4$  epochs to allow the network to reach a steady state. At the end the simulation of each realization, the functions of each node were recorded and then used to calculate the average frequency of each function for the ensemble of realizations.

Figure 1 shows a graph of the attractor period vs. epoch for a simulation of a  $K = 4$  network realization with evolutionary bias  $p = 0.65$ . For the first 6834 epochs all the attractors found have periods longer than  $\Gamma_{\max} = 10^4$ . Then, attractors with shorter periods begin to appear. After about  $10^4$  epochs the network reaches a steady state with a broad distribution of attractor periods. As the figure indicates neither chaotic behavior, exemplified by almost entirely large attractor periods, nor frozen behavior, exemplified by almost entirely short periods, dominate the behavior of the steady state. The steady state is instead at the “edge of chaos” and is a critical state. All network realizations for  $p = 0.65$  and

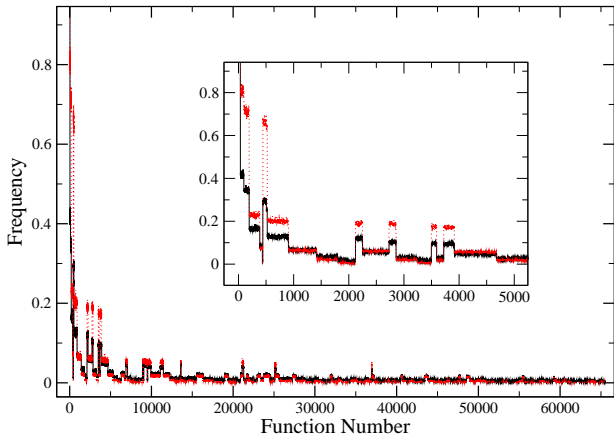


FIG. 2: (Color online) Ensemble averaged frequency of  $K = 4$  Boolean functions in the evolved critical steady state. The black solid line corresponds to  $p = 0.65$ , and the red dotted line corresponds to  $p = 0.75$ . Functions are grouped together in classes based on hyper-octahedral plus parity symmetry and with groups then ordered according to canalization from high to low. The inset shows the same data for functions 1-5000.

$p = 0.75$  showed similar behavior once reaching a steady state. However, for  $p = 0.5$ , no attractor periods of less than 10,000 were observed for any network realization. That is, unlike in the  $K = 3$  case, the system does not self-organize or evolve into a critical state when removing functions and exchanging them with *unbiased* functions. This indicates that the increased complexity of the more highly connected network disrupts the networks ability to self-organize with unbiased functions.

These results indicate that a phase transition occurs in the evolutionary dynamics as  $p$  is increased. At values of  $p$  below the transition value the evolutionary dynamics do not produce a critical steady state, while at values of  $p$  above the transition, a critical steady state evolves. In fact, a second transition occurs at higher values of  $p$ . At values of  $p$  above this second transition, the evolved state is no longer critical but instead remains in the frozen state. Thus, critical steady states evolve only when the bias of the evolutionary process is within a range.

Note that non-evolutionary  $K = 4$  RBNs are constructed with a critical bias of  $p_c \approx 0.85355$ , according to Eq. 4. This value of  $p_c$  produces networks with an average homogeneity of all Boolean function in the network  $P \approx 0.85358$ . However, the steady state value of  $P$  for networks evolved with a bias of  $p = 0.65$  is  $\approx 0.71$ . Clearly, the critical state of  $K = 4$  evolved networks is significantly different than the critical state of non-evolutionary  $K = 4$  RBNs.

Figure 2 shows the ensemble averaged frequency at which each of the  $2^{2^4} = 65536$  different  $K = 4$  Boolean functions occur in the evolved steady state, for bias parameters  $p = 0.65$  and  $p = 0.75$ . The Boolean functions were ordered by first grouping them by their membership to a particular class under hyper-octahedral plus parity

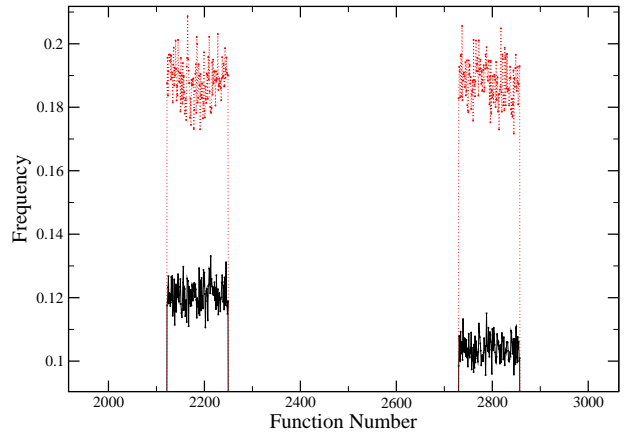


FIG. 3: (Color online) Enlargement of a small portion of Fig. 2. The two classes of functions shown have the same homogeneity but different canalization. Notice that for  $p = 0.65$  (black solid line), the class on the left with higher canalization occurs with a higher frequency than the class on the right with lower canalization. However, for  $p = 0.75$  (red dotted line) both classes occur with approximately the same frequency. This indicates that the bias towards homogeneity is dominating the behavior over the drive for canalization at the high value of bias for these two classes.

symmetry. Then the classes were ordered in descending order by how canalizing the functions in the class are, as measured by the sum of their  $\mathbf{P}_k$  values. As expected, the graph shows that functions belonging to the same class occur with the same probability, at least to within the resolution allowed by statistical fluctuations. This confirms the hypothesis that the underlying symmetry of the evolutionary dynamics is hyper-octahedral plus parity.

Clearly, certain classes of functions occur with a higher probability than others. In general, functions on the left side of the graph (higher canalization) occur much more frequently than functions on the right (lower canalization). However, unlike in the  $K = 3$  case, certain function classes with higher canalization occur less frequently than function classes with lower canalization. This occurs because, unlike in the previous  $K = 3$  studies [17, 23, 24, 26], the evolutionary process here is biased toward homogeneity. In this case, the drive for canalization caused by the evolutionary dynamics is competing against the bias toward homogeneity for certain classes of functions. See Fig. 3. Nonetheless, the evolved critical steady state of these biased networks still shows a preference for canalization and is strikingly different than a critical state of a non-evolutionary RBN where homogeneity entirely dominates the relative frequency of functions.

Analogous results presumably hold for even larger values of  $K$ . However, because the number of Boolean functions for a given  $K$  goes as  $2^{2^K}$ , accurately measuring the frequency that each function occurs at in the critical steady state becomes unfeasible for values of  $K$  greater than 4.

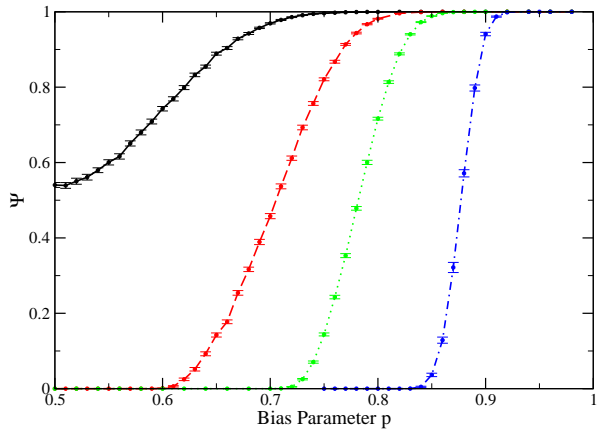


FIG. 4: (Color online) Critical state evolution order parameter  $\Psi$  as a function of evolution bias parameter  $p$  for networks of size  $N = 999$  with  $K = 3$  (black straight line),  $K = 4$  (red dotted line),  $K = 5$  (green dashed line), and  $K = 8$  (blue dashed-dotted line).

### B. Criticality as a function of $p$ and $K$

Our results for  $K = 4$  indicate that canalized critical states evolve only when the bias  $p$  of the evolutionary game is within a range. At too low a value of  $p$ , the evolved steady state is a chaotic state and only long attractor periods are found. At too high a value of  $p$ , the evolved steady state is a frozen state and only short attractor periods are found. Only in an intermediate range of  $p$  does a critical steady state evolve. In order to quantitatively find the approximate range of  $p$  for which critical steady states evolve, we define an order parameter  $\Psi$  as the percentage of steady state attractor periods that occur that are less than  $\Gamma_{max}$ . Then, when  $\Psi = 0$  the networks are assumed to be in the chaotic state, when  $\Psi = 1$  the networks are assumed to be in the frozen state, and when  $0 < \Psi < 1$  the networks are assumed to be in a critical state.

Figure 4 shows a graph of the order parameter  $\Psi$  as a function of the evolution bias parameter  $p$  for network connectivities  $K = 3, 4, 5$ , and  $8$ . This data was produced using networks of size  $N = 999$ , using an equilibration time to reach the steady state of  $10^4$  epochs, and then computing  $\Psi$  over  $3 \times 10^4$  epochs. The  $\Psi$  values were also then averaged over 140 network realizations for each value of  $p$  and  $K$ . (Sixteen realizations were used for  $K = 8$ ). A period cutoff value of  $\Gamma_{max} = 10^4$  was used in these simulations.

For  $K = 3$  the network already evolves to a critical state at  $p = 0.5$ , the smallest possible value of  $p$ , and stops evolving to a critical state at  $p \approx 0.82$ . This is consistent with previous results [17] that unbiased  $K = 3$  networks evolve to critical states. This is not the case, however, for networks with  $K > 3$ . As shown in Fig. 4, the onset of evolution to criticality for these more highly connected networks occurs at a value  $p > 0.5$ . At least

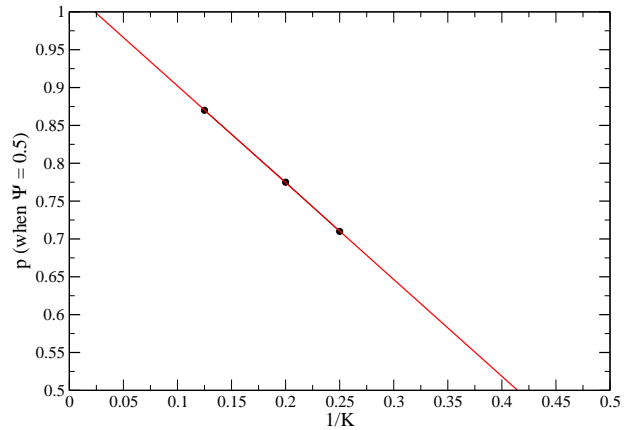


FIG. 5: (Color online)  $p$  when  $\Psi = 0.5$  as a function of  $1/K$  for  $K = 4, 5, 8$ . The straight (red) line is a linear fit to these three data points.

for  $K = 4, 5$ , and  $8$ , and presumably for all finite values of  $K$ , evolution to a critical state occurs only for a finite range of  $p$ . For example, for  $K = 4$ , this range is from  $p \approx 0.60$  to  $p \approx 0.83$ . The width of this range appears to decrease, and both the minimum and median values of  $p$  appear to increase, as  $K$  increases. The findings from the results shown in Fig. 4 vary quantitatively, but remain qualitatively consistent if 1) the equilibration time is increased, 2) the value of  $\Gamma_{max}$  is varied, or 3) the number of nodes  $N$  nodes is changed.

Figure 5 shows the value of  $p$  when  $\Psi = 0.5$ , which approximates the median value of  $p$  in the range of the evolution of a critical state, as a function of  $1/K$  for  $K = 4, 5$ , and  $8$ . Unfortunately, simulating networks with  $K \gg 8$  is computationally unfeasible with our methods, and we are thus restricted to predict the asymptotic behavior of these evolutionary random Boolean networks using these relatively small values of  $K$ . The three points fall roughly on a straight line. If we extrapolate the linear fit of the data points, the value of  $p$  tends toward a value slightly larger than 1 in the limit of large  $K$ . However, this is physically unrealizable since  $p$  cannot be larger than 1. Therefore, we expect that as  $K \rightarrow \infty$ , the width of the range of  $p$  for which criticality occurs goes to 0, while the median value of the range goes to 1.

It is important to note that the range of evolution bias parameter  $p$  for which critical state evolves is, at all studied values of  $K$ , less than the critical bias value  $p_c$  for non-evolutionary RBNs given by Eq. 1. Therefore, the critical steady state that results from evolutionary process is different than the critical state of non-evolutionary RBNs. From previous studies of  $K = 3$  networks, and from the results shown in Fig. 2 that were discussed above, the difference is that the evolved critical steady states are more canalized.

## V. DISCUSSION

In this paper we have extended previous work on an EBN model in which the nodes compete in a frustrated game that causes the Boolean functions of the nodes to evolve. The previous studies of this model found that the game causes the system to evolve to a critical steady state that is highly canalized. Canalized states and their evolutionary mechanisms are important in Developmental Biology because of the usefulness of the robustness against dilute phenotypic expression that canalization in the genome provides. The previous studies also found that the evolutionary dynamics of the  $K = 3$  model has the symmetry of the 3-dimensional Zyklenzeiger group, which is the combination of parity and the cubic symmetry group.

The previous studies of this EBN, however, only considered networks with  $K = 3$  in-links per node. Here we extended the study to the more highly connected networks with larger  $K$ . Real self-regulatory systems, both biological and engineered, typically have nodes with a range of  $K$  inputs [3]. Thus, it is important to understand how larger regulatory connectivity effects evolutionary mechanisms.

For networks with  $K > 3$ , we find that the game as previously studied does not cause the network to evolve to a critical steady state. Instead, it will evolve to a chaotic steady state. This occurs because the unbiased game, which was studied previously, replaces the Boolean function of nodes that lose the game with randomly selected new functions that are chosen unbiasedly from

the set of all possible Boolean functions. Apparently, for networks with  $K > 3$ , unlike what happens for networks with  $K = 3$ , if they are composed largely of nodes with random Boolean functions with an unbiased distribution, then the evolutionary game is not “strong enough” to induce a shift in the distribution of the nodes’ Boolean functions sufficient to have critical state dynamics.

However, we have shown that for networks with  $K > 3$  if the game replaces the Boolean function of the losing nodes with functions biased toward homogeneity, then a critical steady state can evolve. We studied the range of evolutionary bias that will cause critical state evolution and found that it narrows and that its median increases with  $K$ . We have also shown that the critical steady states that evolve for  $K > 3$  are highly canalized, although there is also a competing bias toward more homogeneous Boolean functions. All functions in an orbit of the  $K$ -dimensional Zyklenzeiger group have both equal canalization and equal homogeneity and occur with equal frequency in the steady state. Thus, the symmetry of the evolutionary dynamics of the EBN with  $K$  regulatory links per node is that of the  $K$ -dimensional Zyklenzeiger group.

This study illustrates the importance of symmetry in self-regulatory networks and of evolutionary processes. It would be interesting to analyze other self-regulatory network systems, both real and model systems, with the methods we have used. This would allow the importance of symmetry in evolutionary processes to be understood and become better appreciated.

- 
- [1] S.A. Kauffman, *J. Theor. Biol.* **22**, 437 (1969).
  - [2] S.A. Kauffman, *The Origins of Order* (Oxford University Press, New York, 1993)
  - [3] M. Aldana, S. Coppersmith, and L.P. Kadanoff, in *Perspectives and Problems in Nonlinear Science*, edited by K. Kaplan, J. Marsden, and K. Sreenivasan (Springer-Verlag, Berlin, 2003).
  - [4] B. Drossel, in *Reviews of Nonlinear Dynamics and Complexity*, edited by H.G. Schuster (Wiley-VCH, Berlin, 2008).
  - [5] S. Bornholdt, *Science* **310**, 449 (2005).
  - [6] R. Albert, and H. H. Othmer, *J. Theor. Biol.* **223**, 1 (2003).
  - [7] F. Li, T. Long, Y. Lu, Q. Quyang, and C. Tang, *Proc. Natl. Acad. Sci. U.S.A.* **101**, 4781 (2004).
  - [8] I. Shmulevich, S. A. Kauffman, and M. Aldana, *Proc. Natl. Acad. Sci. U.S.A.* **102**, 13439 (2005).
  - [9] K.Y. Lau, S. Ganguli, and C. Tang, *Phys. Rev. E* **75**, 051907 (2007).
  - [10] B. Derrida and Y. Pomeau, *Europhys. Lett.* **1**, 45 (1986).
  - [11] B. Derrida and G. Weisbuch, *J. Phys. (France)* **47**, 1297 (1986).
  - [12] H. Flyvbjerg, *J. Phys. A* **21**, L955 (1988).
  - [13] I. Shmulevich and S.A. Kauffman, *Phys. Rev. Lett.* **93**, 048701 (2004).
  - [14] U. Bastolla and G. Parisi, *J. Theor. Biol.* **187**, 117 (1997).
  - [15] A. Bhattacharjya and S. Liang, *Phys. Rev. Lett.* **77**, 1644 (1996).
  - [16] F. Greil and K.E. Bassler (2009), arXiv:0911.2481.
  - [17] M. Paczuski, K.E. Bassler, and A. Corral, *Phys. Rev. Lett.* **84**, 3185 (2000).
  - [18] S.A. Kauffman and R.G. Smith, *Physica D* **22**, 68 (1986).
  - [19] S. Bornholdt and K. Sneppen, *Phys. Rev. Lett.* **81**, 236 (1998).
  - [20] S. Bornholdt and T. Rohlf, *Phys. Rev. Lett.* **84**, 6114 (2000).
  - [21] S. Bornholdt and K. Sneppen, *Proc. R. Soc. Lond. B* **267**, 2281 (2000).
  - [22] B. Luque, F.J. Ballesteros, and E.M. Muro, *Phys. Rev. E* **63**, 051913 (2001).
  - [23] K.E. Bassler, C. Lee, and Y. Lee, *Phys. Rev. Lett.* **93**, 038101 (2004).
  - [24] K.E. Bassler and M. Liu, in *Noise in Complex Systems and Stochastic Dynamics III, Proc. of SPIE Vol. 5845*, edited by L.B. Kish, K. Lindenberg, and Z. Gingl (SPIE, Bellingham, WA, 2005).
  - [25] M. Liu and K.E. Bassler, *Phys. Rev. E* **74**, 041910 (2006).
  - [26] M. Liu and K.E. Bassler, *J. Phys. A* **44**, 045101 (2011).
  - [27] A. Szejka and B. Drossel, *Eur. Phys. J. B* **56**, 373 (2007).
  - [28] T. Rohlf, *Europhys. Lett.* **84**, 10004 (2008).

- [29] S. Braunewell and S. Bornholdt, Phys. Rev. E **77**, 060902 (2008).
- [30] T. Mihaljev, and B. Drossel, Eur. Phys. J. B **67**, 259 (2009).
- [31] A. Szejka and B. Drossel, Phys. Rev. E **81**, 021908 (2010).
- [32] C. Priester, A. Szejka, and B. Drossel, Eur. Phys. J. B **80**, 195 (2011).
- [33] D. Challet and Y.C. Zhang, Physica A **246**, 407 (1997).
- [34] C. Waddington, Nature **150**, 563 (1942).
- [35] R. Rutherford and S. Lindquist, Nature **396**, 336 (1998).
- [36] C. Quetsch, T. A. Sangster, and S. Lindquist, Nature **417**, 618 (2002).
- [37] A. Bergman and M. Sigan, Nature **424**, 549 (2003).
- [38] A. Wagner, *Robustness and Evolvability in Living Systems* (Princeton University Press, New Jersey, 2005).
- [39] C. J. O. Reichhardt and K. E. Bassler, J. Phys. A: Math. Theor. **40**, 4339 (2007).
- [40] W.B. Arthur, Am. Econ. Rev. **84**, 406 (1994).
- [41] P. Bak and K. Sneppen, Phys. Rev. Lett. **71**, 4083 (1993).
- [42] T. Gross and B. Blasius, J. R. Soc. Interface **5**, (2008).
- [43] G. Pólya, Acta. Math. **38**, 145 (1937).
- [44] M.A. Harrison, SIAM **11**, 806 (1963).